Shashi and Rana, 2016
J. basic appl. Res 2(3): 266-271

JBAAR
Journal of Basic And Applied Research
ISSN 2413-7014

Ultrastructural Study of Muscle Fibers in Experimental Fluorosis

Shashi A*, Nidhi Rana

Department of Zoology and Environmental Sciences, Punjabi University, Patiala-147002, Punjab, India

*corresponding author: shashiuniindia@yahoo.co.in

Received: 2-5-2016
Revised: 19-5-2016
Published: 22-5-2016

Keywords:
Albino Rat,
Fluoride,
Microvascular damage,
Skeletal muscle,
Ultrastructure

Abstract: The aim of this study was to evaluate the effect of fluoride on the ultrastructure of skeletal muscle. Wistar albino rats were treated with 300 and 600 mg NaF/ kg bw/day respectively, for 40 days . Group I (Control) was given double distilled water ml/kg bw/day orally for the same period. In control rats, the sarcoplasm was filled with myofibrils and some mitochondria. The sarcomeres showed sarcoplasmic reticulum surrounded by Z- line, A and I-bands. The middle of the sarcomere was marked by M-line situated within lighter H-band. Oval myonucleus with finely dispersed chromatin throughout the nucleoplasm was present. In rats treated with 300 mg NaF/ kg bw/day skeletal muscle showed disorganized myofibrils and disruptions in the continuity of plasma membrane. The undulating sarcolemma and many small electron-lucent vacuoles in the myofibers were noticed. The myofibrils showed disturbed contractile structure with loss of sarcomere organization and indistinguishable. A-band, I-band , and irregular and distorted Z-line with disruption of myofilaments. Irregularly shaped markedly shrunken myonuclei with clumped and marginated chromatin were prominent. The cristae rich mitochondria were larger than those in control. The hypercontraction of myofilaments and mitochondrial swelling were observed in rats given 600 mg NaF/ kg bw/day. The sarcoplasmic reticulum was irregularly dialated forming large electron-lucent areas. The myofibrilar pattern could no longer be distinguished . There was loss of integrity of the basal lamina and plasma membrane, and inflammatory cells were present around the damaged site.

INTRODUCTION

Dental and skeletal lesions are the major clinical feature of endemic fluorosis, which is caused by chronic persistent fluoride exposure through ingestion and most commonly occurs as a result of high fluoride levels in drinking water (Zhou *et al*., 2007). Fluoride has a tendency to accumulate in the organisms if the exposure persists over time, even at low concentration (kebsch *et al*., 2007).

It is now well established that ingestion of fluoride affects not only teeth and bones but also many other organs. Structural and biochemical changes in several soft tissues including muscles have been reported in rats from different doses of fluoride (Shashi *et al*., 2010 ; Shashi and Sharma , 2011)

Skeletal muscle is a complex organ composed of particular cells, multinucleate syncytia gathered in a connective network that peripherally continues with the tendinous structures necessary to transmit contractile force of muscle fibers on bone (Magaudda *et al*., 2004). It is composed of heterogeneous fiber types that vary in contraction velocity, endurance capability and metabolic enzyme profile. Both vascular and nervous factors are particularly important for motor performance. The management of the contractile machinery gathered inside myofibers is strictly linked to the activity of the myonuclei, mitochondria, and the system of T tubules and sarcoplasmic reticulum. Skeletal muscle is a highly differentiated tissue that has the capacity to adapt to extreme fluctuations in its functional state. It is also of importance to survey the non-skeletal tissue involvement in fluoride toxicity, prior to establishing an effective therapeutic measures for fluorosis.

Advances in cell biology have progressed our understanding of those factors that contribute to muscle atrophy. Therefore, the present study was designed to evaluate the toxic effects of fluoride on skeletal muscle ultrastructural changes in rodent model.

MATERIAL AND METHODS

Animals and experimental design

Wistar albino rats (n=30) weighing 150-200g were provided with pelleted rodent feed (Hindustan lever limited , Mumbai, India) and water was supplied *ad libitum*. After a 15 day acclimatisation period, they were randomly divided into 3 groups of 6 animals each. The rats of group 1 served as control and received double distilled water one ml/ kg bw/day via oral gavage orally for 40 days. Group II and III recieved 300 and 600 mg NaF/kg bw/day in their drinking water for the same period respectively.

Sample preparation for TEM

At the end of 40 days, the experimental animals of all groups were sacrificed under ether anaesthesia, and small pieces of muscle tissues were fixed overnight in 2.5% buffered glutaraldehyde at 4^0 C and washed 3-4 times in 0.2 M phosphate buffer . Semi- thin longitudinal sections were cut at 1 µm in thickness using glass knife , stained by 1 % toluidine blue in 1 % borax and examined by light microscope. Ultra–thin sections were cut using ultra – microtome . Then sections were mounted on copper grids and stained with saturated uranyl acetate followed by laed citrate. Ultra-thin sections were examined and photographed by FEI Philips Morgagni 268 D transmission electron microscope.

RESULTS

Group I (control)

In control rats, the sarcoplasm appeared filled with myofibrils arranged parallel to the long axis of the myofiber. The myofibrils showed regular arrangements of alternating light (I) and dark (A) bands. The muscle architecture appeared normal with regular and orderly Z-lines, H zones and M lines. The mitochondria with normal cristae, occurs mostly as pairs, one on each side of Z-line, and sarcoplasma adjacent to nuclei. The sarcoplasmic reticulum was normal in distribution and morphology. Glycogen was present in the the sarcoplasm in the form of coarse granules. The plasma membrane and basal lamina were discernible and interfibrillar spacing within the fibers was orderly (Fig.1.).

Oval myonucleus with finely dispersed chromatin throughout the nucleoplasm was present. The nuclear membrane showed small indentations in its contour. (Fig.2). At a higher magnification, oval nuclei was seen under the sarcolemma with their heterochromatin distributed along the inner surface of the nuclear envelope. The mitochondria and their cristae appeared normal. Also the sarcoplasmic reticulum profiles were recognizable, and the myofibrillar structure was distinct (Fig.3.).

Fast twitch fiber types of the muscle fibers were also observed. Type I fibers were characterized by well-defined myofibrils, especially at the A-band level. Intermyofibrillar mitochondria were present isolated or forming columns, sometimes giving a discontinues appearance to the myofibrils. These mitochondria presented variable shapes ranging from round to elongated. The Z-line was broad and straight (Fig.4.). Type II fibers were closely similar to type I fibers, but exhibited numerous lipid droplets associated with the intermyofibrillar mitochondria (Fig.5.).

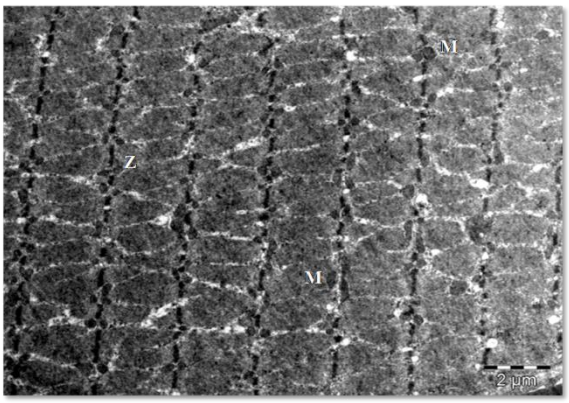

Fig.1. An electron micrograph of a longitudinal section of skeletal muscle of a control rat showing the ultrastructural organization of internal cytoplasmic contents of the cell. Sarcomeres are seen as units bounded by thin, dark lines (Z-lines). Between myofibrils in the intermyofibrillar network, the cell contains glycogen, lipid , mitochondria, and triads. Mitochondria(M) are dark, ovoid structures seen in pairs around the Z-lines. X 1600

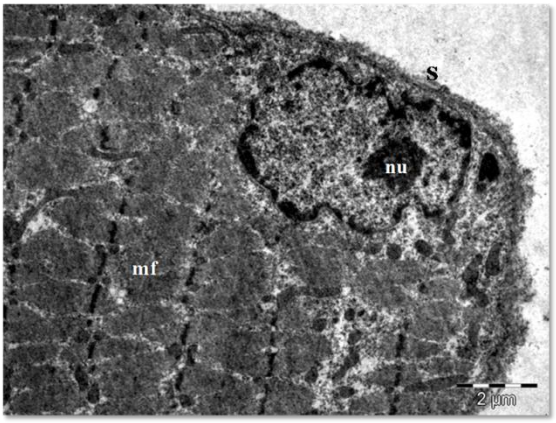

Fig.2. An electron micrograph of a longitudinal section of skeletal muscle of a control rat showing parallel arrangement of myofibrils (mf).The Nucleus lies just beneath the sarcolemma (S) and nucleolus (nu) is also seen. The nucleus contains coarse heterochromatin alternating with euchromatin. X 2000

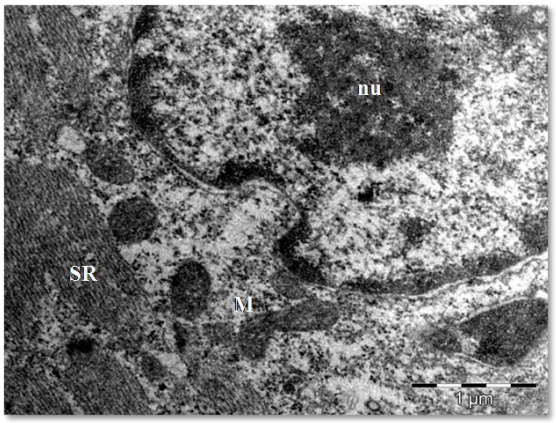

Fig.3. An electron micrograph of a longitudinal section of skeletal muscle of a control rat showing nucleus surrounded by sarcoplasmic reticulum (SR). Mitochondria (M) appeared as dark small circles. X 6300

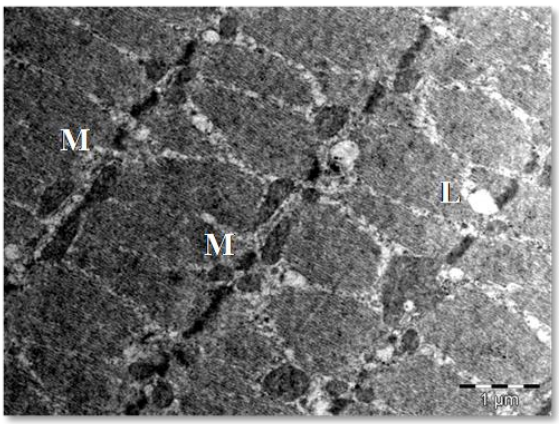

Fig.4. An electron micrograph of a type 1 myofiber in control rat showing abundant and fairly large mitochondria (M). Round, pale gray fairly homogeneous bodies adjacent to the mitochondria are lipid droplets (L). X 4000

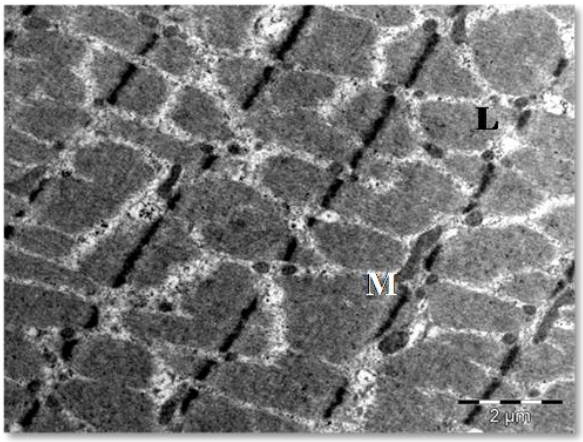

Fig.5. An electron micrograph of a type 2 myofiber in control rat showing the small, less conspicuous mitochondria and low lipid content compared with the type 1 myofiber. X 2500

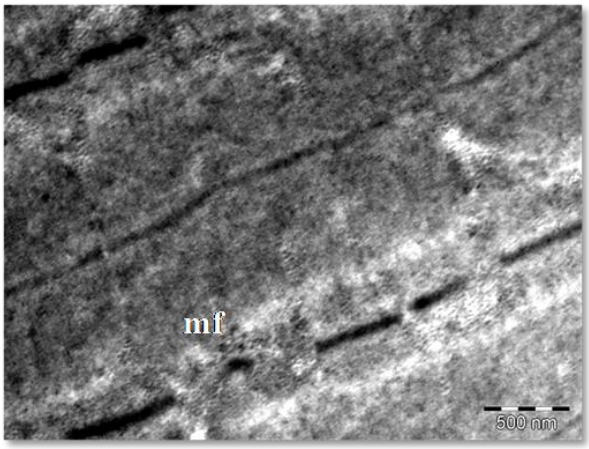

Fig.6. An electron micrograph of a longitudinal section of skeletal muscle of a rat administered 300mg NaF/kg bw/day showing disorganisation and lysis of myofibrils (mf). X 8000

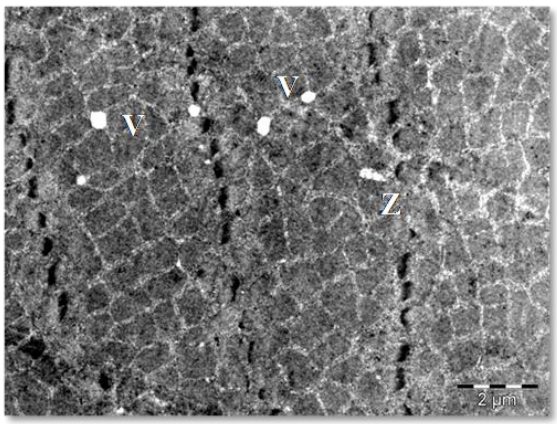

Fig.7. An electron micrograph of a longitudinal section of skeletal muscle of a rat administered 300mg NaF/kg bw/day showing focal disruption of Z-lines and abundant electron-lucent vacuoles (v). X 2000

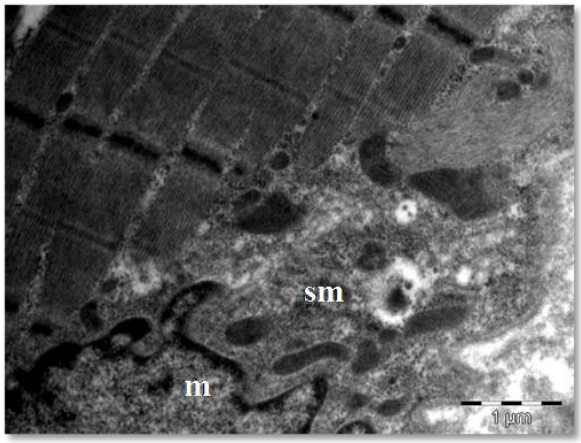

Fig.8. An electron micrograph of a longitudinal section of skeletal muscle of a rat administered 300mg NaF/kg bw/day showing marked aggregation of mitochondria (m) of different shapes and sizes in the subsarcolemmal space (sm). X 5000

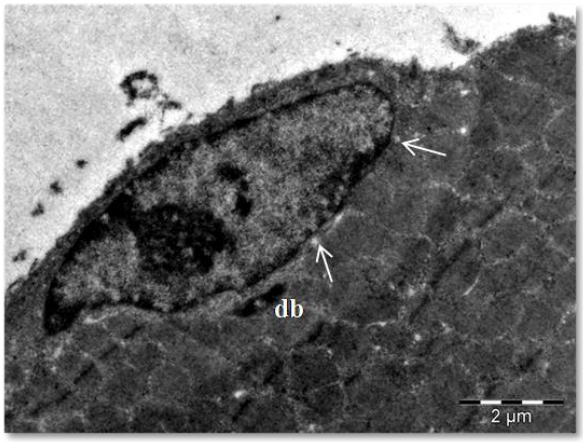

Fig.9. An electron micrograph of a longitudnal section of skeletal muscle of a rat administered 300mg NaF/kg bw/day showing large elongated nucleus (N) with cytoplasm containing dense bodies (db) and pinocytotic vescicles. X 2500

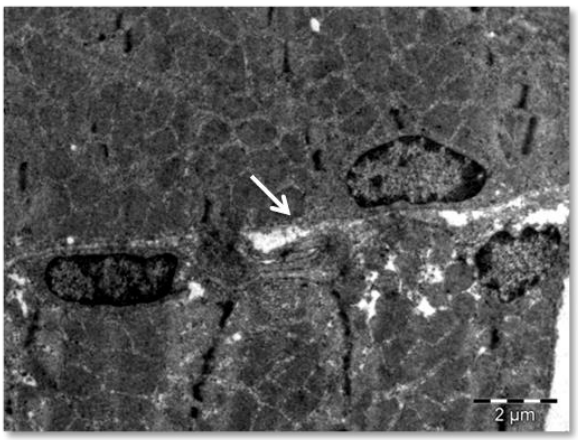

Fig.10. An electron micrograph of a longitudinal section of skeletal muscle of a rat administered 300mg NaF/kg bw/day showing typical myonucleus (M) located inside the sarcolemma of the muscle fiber approaching the site of muscle damage. X 2000

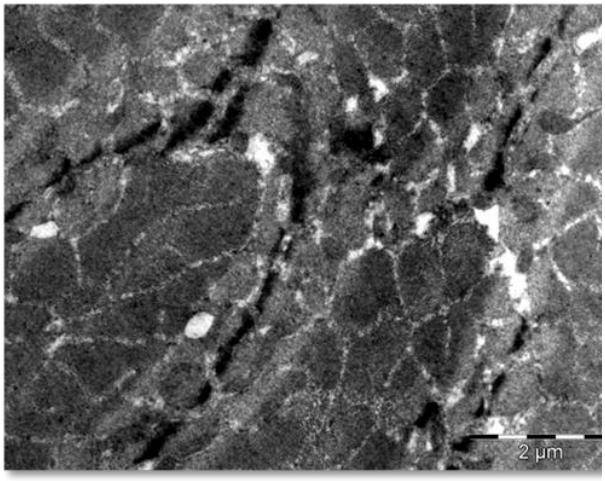

Fig.11. An electron micrograph of a longitudnal section of skeletal muscle of a rat administered 600mg NaF/kg bw/day showing severly disturbed contractile apparatus. X 3200

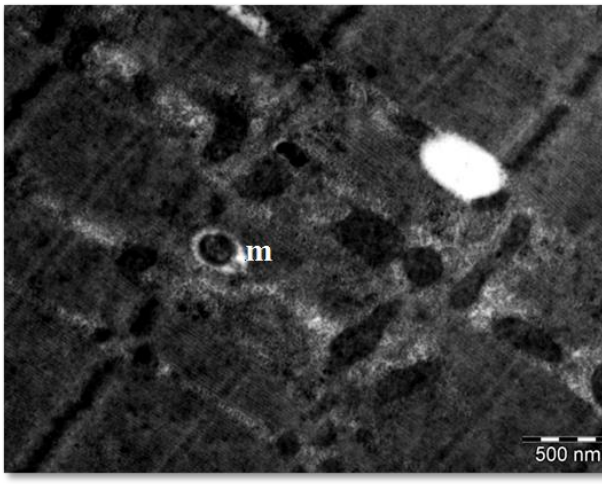

Fig.12. An electron micrograph of a longitudnal section of skeletal muscle of a rat administered 600mg NaF/kg bw/day showing a swolen destroyed mitochondria (m) in the intermyofibrillar space. X 8000

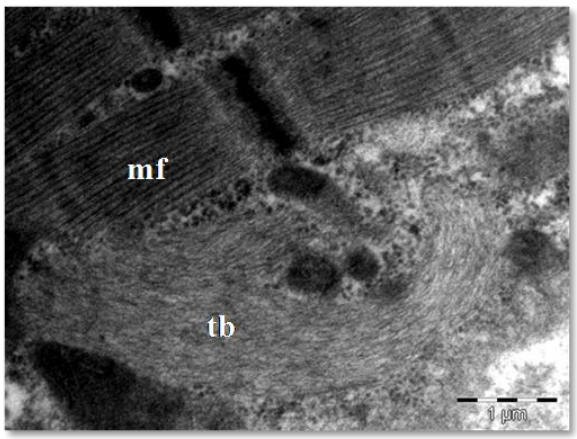

Fig.13. An electron micrograph of a longitudnal section of skeletal muscle of a rat administered 600mg NaF/kg bw/day showing hypercontracted myofibrils (mf). At the periphery tubular aggregates (tb) and modified mitochondria are observed. X 5000

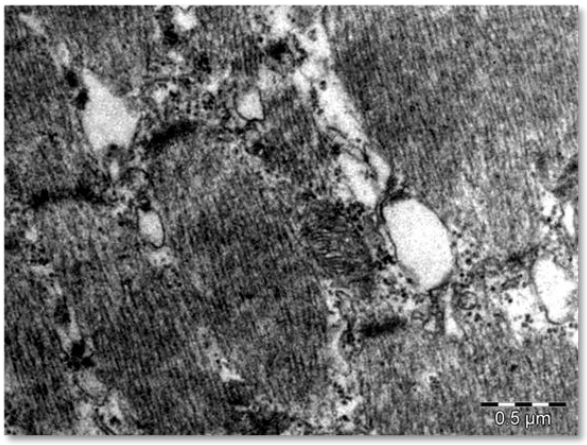

Fig.14. An electron micrograph of a longitudinal section of skeletal muscle of a rat administered 600mg NaF/kg bw/day showing different in size and damaged cristae of mitochondria within an intermyofibrillar space . X 4000

Group II (animals treated with 300 mg NaF/kg bw/day)

The skeletal muscle of rats treated with 300 mg NaF/kg bw/day showed focal disorganization and discontinuation of myofibrils together with focal areas of loss of Z-lines. The areas of myofibrillar disarray with loss of sarcomere pattern were also observed alongwith partial disappearance of light I band and discontinuous Z-line. Many electron–lucent vacuoles and a few dialated vesicles of sarcoplasmic reticulum were also visible (Figs.6, 7). Accumulation of mitochondria of varying sizes and shapes in the subsarcolemmal areas as well as in the intermyofibrillar spaces were markedly prominent (Fig.8.). Irregularly shaped markedly shrunken myonuclei with clumped and marginated chromatin with nearby electron-lucent vacuoles were recorded. The myonuclei showed crenation and folding of the nuclear membrane (Fig.9.). There was loss of integrity of the basal lamina and plasma membrane, and inflammatory cells were present around the damaged site (Fig. 10).

Group III (animals received 600 mg NaF/kg bw/day)

The myofibrils showed severly disturbed contractile structure with loss of sarcomere organization and indistinguishable A-band, I-band , and irregular and distorted Z-line with disruption of myofilaments in rats administered 600 mg NaF/ kg bw/day (Fig. 11).The mitochondrial swelling was prominent. Swollen mitochondria were present among mitochondria that appeared normal. They had small, irregular sized , shaped and ruptured cristae. Fusion of mitochondria to form giant mitochondria was also noticed (Fig. 12). Different degrees of contracted myofibrils were noticed as some sarcomeres showed narrowing or even obliteration of I bands exhibiting hypercontraction (Fig. 13).Mitochondria were shrunken, elongated and irregular with distorted cristae. Glycogen contents were decreased (Fig.14).

DISCUSSION

All examined skeletal muscle samples in the present investigation showed ultrastructural abnormalities. The pathological involvement of muscle fibers, however were not uniform. A wide spectrum of changes were observed on each examined grid. The abnormality most often encountered was the muscle atrophy. The degree of atrophy varied from slight to advanced and corresponded with the intensity of myofibrillar degeneration and involvement of other muscle fiber elements. Both fiber types were affected, as shown by Z-line width. The present finding is in accordance with the study of Kamniska et al (1998) who reported a significant age-dependent functional and morphological deficits in the skeletal muscle of senile rats.

The swelling and rupturing of mitochondria and the disorganization of the sarcoplasmic reticulumn in fluorotic rats suggest a membrane-oriented change. Moreover, disrupted mitochondrial surrounding irregularly shaped myonuclei was noticed in a previous study on immobilized muscles (Smith *et al*., 2000). This coincided with the observation of irregularly shaped markedly shrunken myonuclei with clumped and marginated chromatin by TEM with nearby electron lucent spaces in the cast-immobilized gastrocnemius muscle (Kafoury *et al*., 2011).

Muscles samples from from fluoride treated rats of group II (300mg NaF) revealed widespread mitochondrial swelling with disruption and fragmentation of cristae. Some mitochondrial cristae appeared focally dissolved and poorly organized within swollen mitochondrial membranes. Clumped and focally swollen mitochondrial cristae were found at higher magnification. This was in line with the previously noticed study in the multiple samples of Zidovudine treated rats (Lewis *et al*., 1992).

From the electron microscopy, it can be seen that the membranes of the mitochondria and sarcoplasmic reticulumn were much more sensitive to the fluoride than actual membrane surrounding the muscle cell. Also, the mitochondria located in the middle of the muscle cell , suggesting serae initial changes associated with the sarcolemma.

After fluoride administration, skeletal muscle showed conspicuous damage of muscle fibers. This effect was characterised by alterationss of cell plasma membrane and mitochondrial swelling ,charactersistic features of cell death (Moreira *et al*., 1994). In addition, disruption of basement membrane, which surrounds each muscle fibber, was also observed. This structure is composed of type IV collagen, laminin, nidogen and perlecan, and provides support and regulation of cell behaviour (Rucavado *et al*., 1998). Thus, the degradation of these components, essential for muscle maintainence, could result in disarrangement of muscle fibers induced by fluoride. The myotoxic pathological lesions were reported by the study of Baldo et al (2010) in neuweidase toxicity.

Fluoridated skeletal muscle fibers in group III (600mg NaF) in this study presented undulating sarcolemma, hypercontraction areas, central core-like lesions in the myofibers, electron–lucent vacuoles, myofilament loss in-addition to the loss of sarcomere organization and indistinguishable A-band , I-band , and irregular and distorted Z-line ; all these led to severe disturbed contractile structure of the myofibers. These observations in the fluoride-intoxicated skeletal muscles might be attributed to the signs of the various stages of atrophy process, as a result of promoting disassembly of myofibrillar proteins that anchor myofilaments to the Z-line and maintain sarcomeric alignment. Moreover, sarcomeric disruption, myofilament loss and the vacuolated myofibers were suggested to be a main component of muscle degeneration in the skeletal muscle of immobilized rats (Zarzhevsky *et al*.,1999 ; Gomes *et al*., 2009). The present study revealed widening in the interstitial space in fluoride treated muscle which may be due to myofiberedema (Ferreira *et al*., 2008).

CONCLUSION

It was concluded that fluoride exposure constitutes an insult to the skeletal muscle, suggestive of deleterious microvascular dysfunction.

ACKNOWLEDGEMENTS

The TEM studies were carried out at the Sophisticated Instruments facility for EM at the All India Institute of Medical Sciences (AIIMS), New Delhi, India.

REFERENCES

Barbier , O., Arreola-Mendozab L., &Razoa , L.M.D. (2010). Molecular mechanisms of fluoride toxicity. *Chemico-Biological Interactions*, 188, 319–333.

Baldo ,C. , Ferreira, M.J., Lopes, D.S., Izidoro, L.F.M. , Gomes ,A.O., Ferro, E.A.V., Hamaguchi , A., Homsi-Brandeburgo, M.I ., Rodrigues, V.M. (2010).*The Journal of Venomous Animals and Toxins including Tropical Diseases* ,16 (3) ,462-469.

Ferreira , R., Neuparth, M.J., Vitorino, R., Appell, H.J., Amado, F., Duarte, & J.A . (2008) . Evidences of apoptosis during the early phases of soleus muscle atrophy in hindlimb suspended mice. *Physiology Research*, 57, 601-611.

Gomes, A.R., Cornachione, A., Salvini, T.F ., Mattiello-Sverzut, & A.C. (2007). Morphological effects of two protocols of passive stretch over the immobilized rat soleus muscle. *Journal of Anatomy* , 210, 328-335.

Kaminska , M. A., Gert S , A.F ., Coper, H., Ossowska, K ., Wolfarth, S., &Hausmanowa P , I. (1998). Ultrastructural changes in the skeletal muscle os senile rats significant with age-dependent motor deficits. *Basic Applied Myology*, 8(3) ,185-190.

Kebsch, M., Wilkinson, M., Petocz, P., &Darendeliler, M.A. (2007). The effect of fluoride administration on rat serum osteocalcin expression during orthodontic movemet. *American Journal of Orthodontics and Dentofacial Orthopedics* , 131, 515-524.

Magaudda, L., Mauro D , D., Trimarchi, F., & Anastasi, G. (2004). Effects of physical exercise on skeletal muscle fiber : ultrastructural and molecular aspects. *Basic applied Myology*, 14 (1), 17-21.

Moreira, L., Borkow, G., Ovadia, M., & Gutiérrez, J.M. (1994) Pathological changes induced by BaH1, a hemorrhagic proteinase isolated from *Bothrops asper* (terciopelo) snake venom, on mouse capillary blood vessels. *Toxicon*. 32(8), 977-987.

Rucavado, A., Nunez, J., & Gutierrez, J.M. (1998) . Blister formation and skin induced by BaP1, a haemorrhagic metalloproteinase from the venom of the snake *Bothrops asper*. *International Journal of Experimental Pathology*. 79(4) , 245-254.

Shashi , A., Bhushan, B., & Bhardwaj , M.(2010). Histochemical pattern of gastrocnemius muscle in fluoride toxicity syndrome. *Asian Pacific Journal of Tropical Medicine*. 3(2) , 136-140.

Shashi , A ., & Sharma, N. (2011). The pathology of muscle lesions in experimental fluorosis. *International Journal of Science Innovations and discoveries*, 1(2) , 255-262.

Smith, H.K., Maxwell , L., Martyn, J.A., Bass, J.J. (2000). Nuclear DNA fragmentation and morphological alterations in adult rabbit skeletal muscle after short-term immobilization.*Cell Tissue Research* ,302, 235-241.

Zarzhevsky, N., Coleman, R., Volpin, G., Fuchs, D., Stein, H., &Reznick, AZ .(1999). Muscle recovery after immobilisation by external fixation. *Journal of Bone Joint Surgery*, 81,B,896-901.

Zhou, T., Duan, L.J., Ding, Z., Yang, R.P., & Li SH. (2012). Environmental fluoride exposure and reproductive hormones in male living in endemic fluorosis in China .*Life Science Journal*, 9, 1-7.